



Aalborg Universitet

AALBORG UNIVERSITY
DENMARK

Online Parameter Estimation for Supercapacitor State-of-Energy and State-of-Health Determination in Vehicular Applications

Naseri, Farshid; Farjah, Ebrahim; Ghanbari, Teymoor; Kazemi, Zahra; Schaltz, Erik; Schanen, Jean-Luc

Published in:

I E E E Transactions on Industrial Electronics

DOI (link to publication from Publisher):

[10.1109/TIE.2019.2941151](https://doi.org/10.1109/TIE.2019.2941151)

Publication date:

2020

Document Version

Accepted author manuscript, peer reviewed version

[Link to publication from Aalborg University](#)

Citation for published version (APA):

Naseri, F., Farjah, E., Ghanbari, T., Kazemi, Z., Schaltz, E., & Schanen, J-L. (2020). Online Parameter Estimation for Supercapacitor State-of-Energy and State-of-Health Determination in Vehicular Applications. *I E E E Transactions on Industrial Electronics*, 67(9), 7963-7972. [8844313].
<https://doi.org/10.1109/TIE.2019.2941151>

General rights

Copyright and moral rights for the publications made accessible in the public portal are retained by the authors and/or other copyright owners and it is a condition of accessing publications that users recognise and abide by the legal requirements associated with these rights.

- Users may download and print one copy of any publication from the public portal for the purpose of private study or research.
- You may not further distribute the material or use it for any profit-making activity or commercial gain
- You may freely distribute the URL identifying the publication in the public portal -

Take down policy

If you believe that this document breaches copyright please contact us at vbn@aub.aau.dk providing details, and we will remove access to the work immediately and investigate your claim.

Online Parameter Estimation for Supercapacitor State-of-Energy and State-of-Health Determination in Vehicular Applications

Farshid Naseri, *Student Member, IEEE*, Ebrahim Farjah, *Member, IEEE*, Teymoor Ghanbari, *Member, IEEE*, Zahra Kazemi, *Student Member, IEEE*, Erik Schaltz, *Member, IEEE*, and Jean-Luc Schanen, *Senior Member, IEEE*

Abstract— Online accurate estimation of supercapacitor State-of-Health (SoH) and State-of-Energy (SoE) is essential to achieve efficient energy management and real-time condition monitoring in Electric Vehicle (EV) applications. In this paper, for the first time, Unscented Kalman Filter (UKF) is used for online parameter and state estimation of the supercapacitor. In the proposed method, a nonlinear state-space model of the supercapacitor is developed, which takes the capacitance variation and self-discharge effects into account. The observability of the considered model is analytically confirmed using a graphical approach (GA). The SoH and SoE are then estimated based on the supercapacitor online identified model with the designed UKF. The proposed method provides better estimation accuracy over KF and Extended KF (EKF) algorithms since the linearization errors during the filtering process are avoided. The effectiveness of the proposed approach is demonstrated through several experiments on a laboratory testbed. An overall estimation error below 0.5% is achieved with the proposed method. In addition, Hardware-in-the-Loop (HIL) experiments are conducted and real-time feasibility of the proposed method is guaranteed.

Index Terms— Electric Vehicles (EVs), State-of-Energy (SoE), State-of-Health (SoH), Supercapacitor, Unscented Kalman Filter (UKF).

I. INTRODUCTION

ELECTRIC Double Layer Capacitors (EDLCs), also known as supercapacitors or ultracapacitors, have gained increasing attention from the transportation sector due to their appealing features such as high power density, long cycle life, etc. In vehicular applications, the supercapacitor can be used as a complementary Energy Storage System (ESS) in conjunction with the chemical batteries to improve the vehicle performance during transient states such as acceleration and regenerative braking conditions [1]. For example, ENEA (Italian National Agency for New Technologies, Energy and Sustainable Economic Development) has recently developed an electric bus that actively combines the supercapacitors and batteries in a Hybrid Energy Storage System (HESS), which shows the industrial importance of such systems [2]. However, the performance of the supercapacitor heavily depends on its State-of-Health (SoH) and State-of-Energy (SoE). The SoH and SoE are critical metrics that determine how much energy the

supercapacitor can absorb or release during a particular vehicle state [3]. Therefore, online accurate estimation of the foregoing variables is essential. The estimation accuracy of the SoH and SoE relies on the supercapacitor model fidelity and the estimation algorithm. In fact, an effective estimation method is needed for updating the model parameters in real-time to account for aging effects [4]. Different methods have been proposed for estimation of the supercapacitor SoH and SoE. In the following, a brief review of the state of art is presented:

The basic approach for the estimation of supercapacitor SoH is electrochemical impedance spectroscopy (EIS) [5]–[6]. The EIS is a frequency-based characterization approach, which provides a very accurate estimation of SoH. However, the EIS requires costly instrumentation. More importantly, the EIS is an offline method and is not suitable for vehicular applications, where the estimation algorithm must run online. In [7], the SoH is estimated in an offline manner based on the bias voltage, current, and temperature during cycling tests. Artificial Neural Network (ANN) has been used for SoH estimation in [8]. A frequency spectrometer has been used to obtain some training data in the frequency domain. The main drawback of this approach is that a sufficiently rich dataset is needed for the training phase, which makes its implementation difficult and time-consuming. In [9], Least-Squares (LS) algorithm has been used for the estimation of supercapacitor states. However, the ordinary LS method is not suitable for online execution as its computational burden exponentially increases with the size of the measurement vector. To resolve the foregoing problem, Recursive LS (RLS) algorithm has been used in [10]–[12] for state estimation in the supercapacitors. In [13], an online approach based on the Extended RLS (ERLS) algorithm has been used to account for the undesirable effect of the measurement noises. However, all the foregoing LS-based approaches are designed based on the simple RC model of the supercapacitor, which neglects the self-discharging and charge redistribution effects.

In addition to the SoH, the supercapacitor SoE should also be accurately estimated. The basic approach for estimation of SoE is ampere-hour counting. However, the accuracy of this method is relatively low due to the accumulation of measurement errors over time. To rectify the foregoing problem, an effective SoE estimation approach based on the Luenberger style observer has been proposed in [14]. In this method, based on the difference between the actual and predicted supercapacitor voltages, a feedback loop is employed to compensate for the measurement errors, modeling uncertainties, and numerical computation errors. Another effective observer-based approach based on the generalized extended state observer (GESO) has been proposed for SoH and

Manuscript received April 07, 2019; revised July 25, 2019; accepted August 25, 2019.

F. Naseri, E. Farjah, T. Ghanbari, and Z. Kazemi are with the School of Electrical and Computer Engineering, Shiraz University, Shiraz, Iran (email: f.naseri@shirazu.ac.ir; farjah@shirazu.ac.ir; ghanbarih@shirazu.ac.ir; z.kazemi@shirazu.ac.ir).

E. Schaltz is with the Department of Energy Technology, Aalborg University, Aalborg, Denmark (email: esc@et.aau.dk).

J. -L. Schanen is with the Grenoble Electrical Engineering Lab (G2ELab), Grenoble, France (email: schanen@g2elab.inpg.fr).

SoE estimation in [15]. The three-branch equivalent circuit model of the supercapacitor has been used together with the GESO. However, the effect of the leakage current is omitted in the estimation of SoE. It is noteworthy that the foregoing observer-based methods have relatively low computational burden since they fulfill the state estimation by only using the supercapacitor model. However, the observers are deterministic and thus, they cannot suitably deal with undesirable effects of the measurement noises with stochastic nature. Thus, in vehicular applications where the supercapacitor model parameters experience frequent variations and measurements are subjected to error and noise sources, a state estimation algorithm that has an inherent capability to deal with such modeling uncertainties, measurement errors, and stochastic noises is needed.

To tackle the foregoing problems, KF and EKF-based algorithms have been used for estimation of the supercapacitor states [16]-[18]. In [16] and [18], a three-branch equivalent circuit model of the supercapacitor is considered and Kalman Filter (KF) has been used for estimation of the supercapacitor SoE. The model parameters and SoH are estimated with least mean square error (LMSE) fitting approach and KF is only used for estimation of the voltages across the capacitive branches. The main disadvantage of this approach is that the effect of the leakage current is ignored. Furthermore, the LMSE algorithm used for parameter estimation is not computationally efficient due to the involvement of a heavy matrix inversion process. In addition, the effects of measurement errors and noises cannot be suitably handled during parameter estimation with the LMSE algorithm. In [17], Extended KF (EKF) has been used for estimation of the supercapacitor SoH. The EKF is used for estimation of the aging indicators using an RC equivalent circuit model, which takes into account the capacitance variation effect. At each iteration, the EKF considers a first-order linearization of the supercapacitor nonlinear model, which might lead to sub-optimal performance and sometimes divergence of the filter. In addition, the considered model in [17] does not account for the self-discharging phenomenon of the supercapacitor.

Although there have been various studies for the estimation of supercapacitor SoH and SoE, there are still some points that remain to be addressed. In vehicular applications, where the real-time state estimation is a must, a simplified supercapacitor model with relatively low computational burden is usually preferred. For instance, although the three-branch equivalent circuit model of the supercapacitor exhibits a very good accuracy, it necessitates the use of a separate algorithm for estimation of the supercapacitor unobservable internal state variables, which lowers the computational efficiency. On the other hand, the use of over-simplified supercapacitor models decreases the accuracy of the state estimation. Therefore, a supercapacitor model with moderate complexity can be useful if the state estimator has the inherent capability of effectively dealing with modeling uncertainties. More importantly, the state estimator should be able to handle the inherent sensor errors, sensor drift due to a change in the operating conditions, errors associated with analog to digital conversion (ADC) units, Electromagnetic Interference (EMI) and noise effects, etc. As discussed before, the KF-based filtering methods are best suited for dealing with the stochastic nature of the modeling uncertainties and measurement errors. The filter-based

techniques have also been used for state estimation in other ESS types such as electrochemical batteries, which indicates the usefulness if these estimation tools [19]-[20]. However, the KF and EKF use a linearized supercapacitor model, which decreases the accuracy of the state estimation. In addition, the EKF algorithm has high computational burden since a Jacobian matrix needs to be calculated at each iteration of the algorithm.

To address the mentioned issues, in this paper, for the first time, Unscented KF (UKF) algorithm is used for accurate concurrent estimation of the supercapacitor SoH and SoE. An RC equivalent circuit model of the supercapacitor which effectively takes into account the capacitor variation and self-discharging effects is considered in the UKF algorithm. Unlike other approaches that fulfill the parameter and state estimation in separate steps, the proposed UKF-based approach obtains the supercapacitor SoH and SoE using only one filtering process. The foregoing technique increases the estimation accuracy by taking into account the cross-correlations between the parameters and states. In addition, it has easier implementation since only one filtering algorithm is needed. The main features of the proposed approach are highlighted as follows:

- 1- This work is the first attempt for using UKF in joint estimation of the supercapacitor SoH and SoE. The UKF provides better accuracy over existing methods such as EKF but remarkably, the computational complexity of the UKF is lower than the EKF, as will be proved later.
- 2- The capacitance variation and self-discharging effects are considered in the supercapacitor model.
- 3- Both the SoH and SoE are estimated using a single UKF-based filtering process, which is accomplished by augmenting the internal voltage of the supercapacitor as a new state variable with the main system model.
- 4- The real-time feasibility of the proposed UKF-based approach is demonstrated by a series of Hardware-in-the-Loop (HIL) experiments.

The rest of the paper is structured as follows: In [Section II](#), the operating principles of the proposed method is presented. In [Section III](#), the experimental results of the proposed approach on an implemented testbed are provided and discussed. To demonstrate the real-time feasibility of the proposed method, some HIL experiments are conducted and the results are reported in [Section IV](#). In [Section V](#), the proposed approach is compared with the KF-based and EKF-based algorithms in terms of accuracy and computational complexity. Finally, the main results are concluded in [Section VI](#). An [APPENDIX](#) provides some details regarding the implemented algorithm.

II. OPERATING PRINCIPLES OF THE PROPOSED METHOD

The key step for accurate estimation of the SoH and SoE lies in the precise parameter estimation and successful observation of the supercapacitor internal voltage. In this paper, both the parameter and internal state estimation tasks are fulfilled using the proposed UKF-based approach. Different steps of the proposed method are explained in the following subsections.

A. Problem statement

The target of this paper is to develop an online, accurate, and computationally friendly SoH and SoE indicator. It is assumed that the supercapacitor measurable parameters are its

terminal voltage and charge/discharge current. The equivalent series resistance R_s and the internal capacitance C are considered as the key signatures for indicating the supercapacitor SoH. According to the estimates of the foregoing parameters, the supercapacitor SoH can then be quantified based on an End-of-Life (EoL) criterion. For example, according to IEC-62391, the supercapacitor reaches its EoL when the ESR increases by two times of the rated ESR. Therefore, the SoH can be calculated as follows:

$$SoH(\%) = \frac{2ESR_{rated} - ESR_{estimated}}{ESR_{rated}} \times 100 \quad (1)$$

where ESR_{rated} and $ESR_{estimated}$ are the rated and estimated ESR values, respectively. In addition, SoE is defined as the remaining energy, which is shown in percentage. The stored energy of the supercapacitor can be given by:

$$E = \int Q dv_c = \int C v_c dv_c = \int C v_c^2 dv_c = \frac{1}{2} C v_c^2 + \frac{1}{3} C v_c^3 \quad (2)$$

where E is the stored energy in Joules, Q is the electric charge, C is the internal capacitance, and v_c is the estimated internal voltage of the supercapacitor. The SoE is calculated as the ratio of the remaining energy to the maximum energy of the supercapacitor E_{max} in percentage:

$$SoE(\%) = \frac{E}{E_{max}} \times 100 \quad (3)$$

The maximum energy E_{max} is derived when the supercapacitor internal voltage v_c equals to the rated supercapacitor voltage V_{rated} . Therefore, the accurate estimation of SoH and SoE relies on the precise estimation of the supercapacitor internal voltage and its model parameters.

B. Supercapacitor nonlinear state-space model

In this paper, a first-order equivalent circuit model of the supercapacitor is used. In order to effectively mimic the supercapacitor real behavior, the capacitance variation and charge redistribution effects are taken into account. The considered model is shown in Fig. 1, in which U_c , i , and v_c are the terminal voltage, current, and supercapacitor internal voltage, respectively. In addition, R_s is the equivalent series resistance (ESR), R_p is the equivalent parallel resistance (EPR), and C is the supercapacitor voltage-dependent capacitance, which is described with the following expression [21]-[22]:

$$C = g(v_c) = C_0 + C_1 v_c \quad (4)$$

In (4), C_0 is a constant capacitance. In addition, it can be assumed that the capacitance C linearly evolves with an almost constant or a slow time-varying slope and thus, $dC_1/dt \approx 0$. The voltage across the supercapacitor internal capacitance can be written as:

$$v_c = \frac{1}{C} \int (i - \frac{v_c}{R_p}) dt \quad (5)$$

The supercapacitor internal voltage v_c is considered as the first state variable ($x_1 = v_c$). Taking the derivative of (5), one can write:

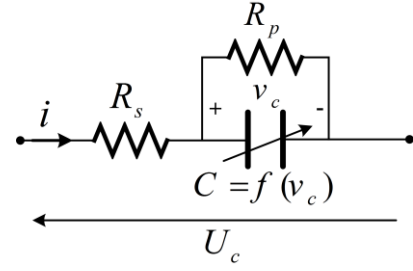


Fig. 1. RC equivalent circuit model of the supercapacitor considering the self-discharge and capacitance variation effects

$$\begin{aligned} \frac{dv_c}{dt} &= \frac{d}{dt} \left(\frac{1}{C} \right) \int (i - \frac{v_c}{R_p}) dt + \frac{1}{C} (i - \frac{v_c}{R_p}) = \\ &= \frac{d}{dt} \left(\frac{1}{C} \right) \int i dt - \frac{1}{R_p} \frac{d}{dt} \left(\frac{1}{C} \right) \int v_c dt + \frac{1}{C} (i - \frac{v_c}{R_p}) \end{aligned} \quad (6)$$

The integration of v_c is also considered as a second state variable ($x_2 = \int v_c dt$). From (4) and (6), dC/dt can be written as follows:

$$\frac{dC}{dt} = C_1 \frac{dv_c}{dt} = C_1 \left(\frac{d}{dt} \left(\frac{1}{C} \right) \int i dt - \frac{1}{R_p} \frac{d}{dt} \left(\frac{1}{C} \right) x_2 + \frac{1}{C} (i - \frac{x_1}{R_p}) \right) \quad (7)$$

Considering $1/C$ as a state variable and using (7), the derivative of $1/C$ can be obtained as follows:

$$\begin{aligned} \frac{d}{dt} \left(\frac{1}{C} \right) &= \frac{-1}{C^2} \frac{dC}{dt} = \frac{-1}{C^2} C_1 \left(\frac{d}{dt} \left(\frac{1}{C} \right) \int i dt - \frac{1}{R_p} \frac{d}{dt} \left(\frac{1}{C} \right) x_2 + \frac{1}{C} (i - \frac{x_1}{R_p}) \right) \\ &= \frac{-C_1}{C^2} \frac{d}{dt} \left(\frac{1}{C} \right) \int i dt + \frac{C_1 x_2}{C^2 R_p} \frac{d}{dt} \left(\frac{1}{C} \right) - \frac{C_1}{C^3} (i - \frac{x_1}{R_p}) \end{aligned} \quad (8)$$

With some manipulations, the following state equation can be derived:

$$\begin{aligned} \frac{d}{dt} \left(\frac{1}{C} \right) \left[1 + \frac{C_1}{C^2} \int i dt - \frac{C_1 x_2}{C^2 R_p} \right] &= -\frac{C_1}{C^3} (i - \frac{x_1}{R_p}) \Rightarrow \frac{d}{dt} \left(\frac{1}{C} \right) = \\ &= \frac{1}{A} \frac{-C_1}{C^3} (i - \frac{x_1}{R_p}) \end{aligned} \quad (9)$$

The supercapacitor voltage U_c is considered as the system output y as follows:

$$y = U_c = R_s i + v_c \quad (10)$$

where the supercapacitor current i is considered as the system input u . The state vector is then considered as follows:

$$X = [x_1 \ x_2 \ x_3 \ x_4 \ x_5 \ x_6 \ x_7]^T = [v_c \ \int v_c \ R_s \ R_p \ C_1 \ \frac{1}{C} \ y]^T \quad (11)$$

In (11), the parameters R_s , R_p , and C_1 are also considered as state variables and since these parameters have a slowly time-varying nature, the following state equations can be deduced:

$$\begin{aligned} x_3 = R_s \rightarrow \dot{x}_3 &= 0, \quad x_4 = R_p \rightarrow \dot{x}_4 = 0 \\ x_5 = C_1 \rightarrow \dot{x}_5 &= 0 \end{aligned} \quad (12)$$

Considering (4)-(9), other state-space equations can be written as follows:

$$\dot{x}_1 = \left(\frac{-1}{1 + x_5 x_6^2 \int u dt - (x_6^2 x_5 x_2) / x_4} \right) x_5 x_6^2 \left(u - \frac{x_1}{x_4} \right) \times \left(\int u dt - \frac{x_2}{x_4} \right) + x_6 \left(u - \frac{x_1}{x_4} \right) \quad (13)$$

$$\dot{x}_2 = x_1 \quad (14)$$

$$\dot{x}_6 = \left(\frac{-1}{1 + x_5 x_6^2 \int u dt - (x_6^2 x_5 x_2) / x_4} \right) x_5 x_6^3 \left(u - \frac{x_1}{x_4} \right) \quad (15)$$

As seen in (11), the system output ($y = U_c$) is also considered as a state variable. In the next subsection, it is explained that $x_7 = y$ is considered to ensure the model observability in all operating conditions. Hence, the last state-space equation can be derived as follows:

$$x_7 = y \xrightarrow{\text{From (7)}} \dot{x}_7 = \dot{y} = \dot{x}_3 u + x_3 \dot{u} + \dot{x}_1 = x_3 \dot{u} + \dot{x}_1 \quad (16)$$

where \dot{x}_1 should be substituted from (13).

C. Observability of the system

In this paper, the system observability is demonstrated using an innovative Graphical Approach (GA) recently proposed by Liu *et al.* [23]. In this approach, the dynamic interdependence between the system states will be exploited through a so-called inference diagram. The system inference diagram is obtained through the following steps: 1- If x_j appears in the differential equation of x_i , a direct link $x_i \rightarrow x_j$ is drawn, which implies that the information on x_j can be collected by monitoring x_i as a function of time. The inference diagram for the considered system is shown in Fig. 2. 2- The obtained inference diagram is then decomposed into a unique set of maximal strongly connected components (SCCs). The SCCs are the largest subgraphs selected such that there is a straight path from each node to all other nodes in that subgraph. The SCCs are surrounded by the red dashed circles in Fig. 2. 3- The SCCs that have no incoming edges are defined as root SCCs (RSCCs).

Definition 1: The necessary and sufficient condition for observability of all system states is that in the inference diagram, at least one node from each RSCC is a sensory node [23].

As seen in Fig. 2, only one RSCC exists in the system inference diagram. The RSCC includes the state variable x_7 , which is equal to the supercapacitor measured terminal voltage. Therefore, since RSCC includes a sensory node, based on Definition 1, the observability of the whole system can be guaranteed [23].

In this paper, the supercapacitor model consisting of (12)-(16) are used for supercapacitor SoH and SoE estimation and sufficiently good results are obtained. However, more complicated supercapacitor models such as the three-branch equivalent circuit model can also be used with the proposed UKF-based approach to further improve the estimation accuracy.

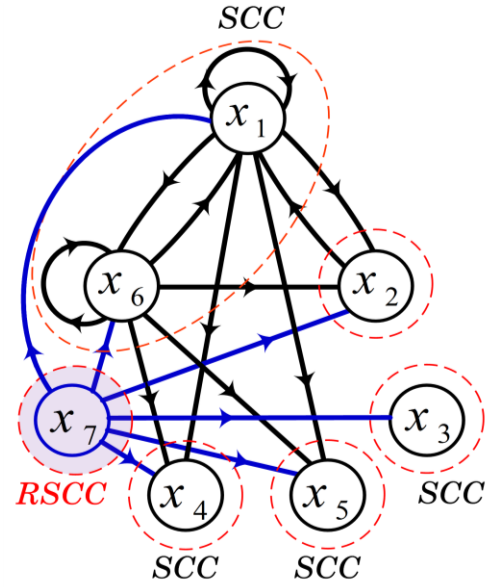


Fig. 2. Inference diagram of the supercapacitor internal states. The sensory node indicated with blue color is related to the supercapacitor terminal voltage U_c . Balance equations of x_1 to x_7 are represented by (12)-(16).

D. The proposed UKF-based SoH and SoE indicator

The UKF algorithm has been widely used for state estimation. Unlike the EKF which involves a linearization stage through the calculation of a Jacobian matrix (partial derivative matrices), the UKF has less computational effort as it does not depend on Jacobians [24]-[26]. In a general case, the discrete-time state-space representation of the supercapacitor model can be expressed as follows:

$$\begin{aligned} X_{k+1} &= f(X_k, u_k, t_k) + \omega_k \\ y_k &= h(X_k, t_k) + v_k \\ \omega_k &\sim (0, Q_k) \\ v_k &\sim (0, R_k) \end{aligned} \quad (17)$$

where X_k is the state vector at sample k , u is the system input (supercapacitor current), ω is the process noise, and v is the measurement noise. The process and measurement noises are considered to be uncorrelated Gaussian white noises, which are included to account for the modeling uncertainties and measurement errors. In the first two formulas of (17), $f(\cdot)$ and $h(\cdot)$ are nonlinear functions, which express alternative representations of the system model (12)-(16). The third and fourth formulas in (17) show that the process and measurement noises have zero mean and covariance matrices $Q^{7 \times 7}$ and $R^{1 \times 1}$, respectively. At the first step, the UKF algorithm is initialized by assigning initial values to the system states (\hat{X}_0^+) and the covariance matrix of the estimation error (P_0^+). The covariance matrix P exhibits the uncertainty in the estimated system states. The initializing process is only fulfilled at the first iteration ($k=1$). The UKF algorithm performs a nonlinear transformation (unscented transform) on a series of the so-called sigma points in state space whose probability density function (PDF) suitably approximates the true PDF of the state vector. In the considered supercapacitor model, there exist $m=7$ state variables and thus, $2m=14$ different sigma points are selected as follows [27]:

$$\begin{aligned}\tilde{X}^{(i)} &= (\sqrt{7P_{k-1}^+})_i^T, i = 1, 2, \dots, 7 \\ \tilde{X}^{(i+7)} &= -(\sqrt{7P_{k-1}^+})_i^T, i = 1, 2, \dots, 7 \\ \hat{X}_{k-1}^{(i)} &= \hat{X}_{k-1}^- + \tilde{X}^{(i)}, i = 1, 2, \dots, 14\end{aligned}\quad (18)$$

Then, the known nonlinear supercapacitor model $f(\cdot)$ is used to transform the sigma points into $\hat{X}_k^{(i)}$ vectors as follows:

$$\hat{X}_k^{(i)} = f(\hat{X}_{k-1}^{(i)}, u_k, t_k) \quad (19)$$

The time update phase for obtaining the *a priori* state estimates and the covariance matrix of the estimation error is fulfilled using the following expressions:

$$\begin{aligned}\hat{X}_k^- &= \frac{1}{14} \sum_{i=1}^{14} \hat{X}_k^{(i)} \\ P_k^- &= \frac{1}{14} \sum_{i=1}^{14} (\hat{X}_k^{(i)} - \hat{X}_k^-)(\hat{X}_k^{(i)} - \hat{X}_k^-)^T + Q_{k-1}\end{aligned}\quad (20)$$

where \hat{X}_k^- is the *priori* estimation up to the sample k . Next, the measurement update phase is fulfilled considering a new set of sigma points as follows:

$$\begin{aligned}\tilde{X}^{(i)} &= (\sqrt{7P_k^-})_i^T, i = 1, 2, \dots, 7 \\ \tilde{X}^{(i+7)} &= -(\sqrt{7P_k^-})_i^T, i = 1, 2, \dots, 7 \\ \hat{X}_k^{(i)} &= \hat{X}_k^- + \tilde{X}^{(i)}, i = 1, 2, \dots, 7\end{aligned}\quad (21)$$

It should be noted that the same sigma points of (18) (from the time update phase) can be reused during the measurement update phase to further save the computational effort, which is of great importance for real-time vehicular applications [27]. The known nonlinear output equation $h(\cdot)$ is subsequently used to transform the sigma points (21) into $\hat{y}_k^{(i)}$ vectors as follows:

$$\hat{y}_k^{(i)} = h(\hat{X}_k^{(i)}, t_k) \quad (22)$$

In order to calculate the predicted measurement and its covariance matrix at time k , the following formulas are used:

$$\begin{aligned}\hat{y}_k &= \frac{1}{14} \sum_{i=1}^{14} \hat{y}_k^{(i)} \\ P_y &= \frac{1}{14} \sum_{i=1}^{14} (\hat{y}_k - \hat{y}_k^{(i)})(\hat{y}_k - \hat{y}_k^{(i)})^T + R_k\end{aligned}\quad (23)$$

Note that R_k is added in the second formula of (23) to account for the effect of measurement noise. The cross-covariance between \hat{y}_k and \hat{X}_k^- can also be obtained as follows:

$$P_{xy} = \frac{1}{14} \sum_{i=1}^{14} (\hat{X}_k^{(i)} - \hat{X}_k^-)(\hat{y}_k^{(i)} - \hat{y}_k)^T \quad (24)$$

Finally, the measurement at instant k is taken into account during the measurement update step as follows:

$$\begin{aligned}K_k \text{ (Kalman Gain)} &= P_{xy} P_y^{-1} \\ \hat{X}_k^+ &= \hat{X}_k^- + K_k (y_k - \hat{y}_k) \\ P_k^+ &= P_k^- - K_k P_y K_k^T\end{aligned}\quad (25)$$

The second formula of (25) gives the final state estimates, in which \hat{x}_{3k}^+ and \hat{x}_{6k}^+ are the supercapacitor SoH indicators. In addition, \hat{x}_{1k}^+ can be used to calculate the SoE using (2)-(3). The whole algorithm flow of the proposed approach is illustrated in Fig. 3.

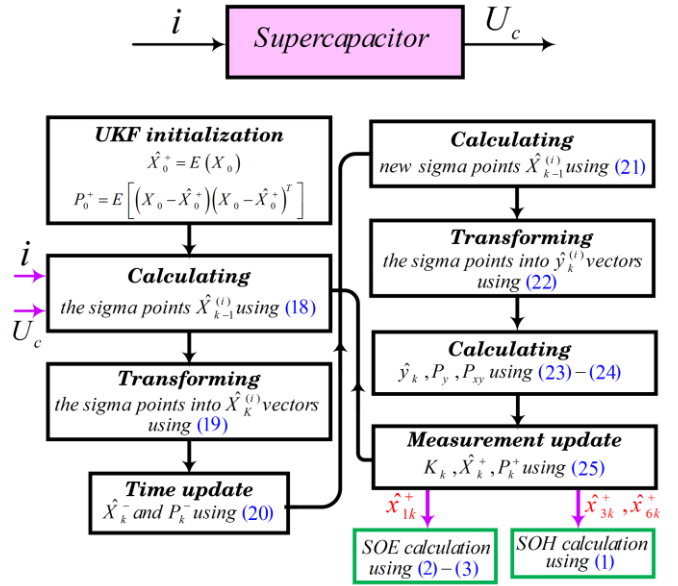


Fig. 3. Flowchart of the proposed UKF-based SoE and SoH estimation approach

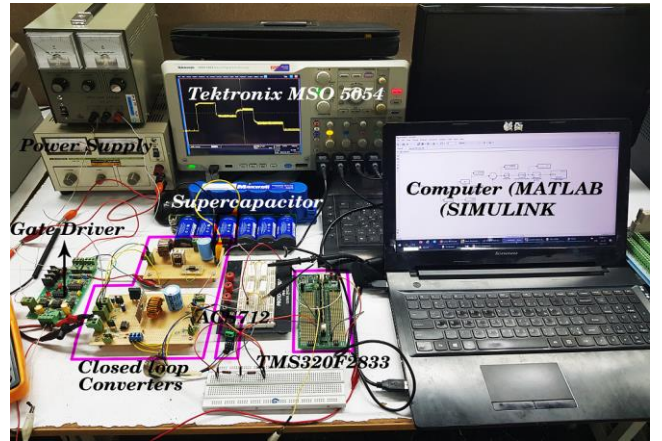


Fig. 4. Experimental testbench for testing the proposed UKF-based approach

E. Settings of the proposed UKF-based approach

As explained before, the state estimator must be initialized at the first iteration ($k=1$). In order to demonstrate the merits of the proposed approach more intuitively, it is herein assumed that no initial information about the system states is available. Therefore, the initial values of x_1 to x_7 and the covariance matrix of the estimation error are set as follows:

$$\begin{aligned}\hat{X}_0^+ &= 0^{7 \times 1} \\ P_0^+ &= 10 \times I^{7 \times 7}\end{aligned}$$

where 0 and I are zero and identity matrices, respectively. However, in order to increase the filter convergence speed, the initial values of the state variables can be set to their rated values, most of which are known from the supercapacitor datasheet or by a standard offline test. The covariance matrices of the process and measurement noises reflect the accuracy levels of the sensor measurements as well as the considered supercapacitor model. The covariance matrix of the measurement noise is chosen based on the typical errors of the voltage sensor as well as the ADC units. In addition, the

diagonal covariance matrix of the process noise is selected with trial and error. These matrices are assigned as follows:

$$R = 0.015, Q = \text{diag}(0.1, 0.1, 0.1, 0.5, 0.3, 0.1, 0.2)$$

More theoretic information about the optimal selection of the covariance matrices of the measurement noise and process noise can be found in [27].

III. EXPERIMENTAL RESULTS

In order to assess the performance of the proposed method, several experiments are conducted and the results are presented in this Section. In the following, the experimental testbed is introduced and the results are discussed in details.

A. Description of the implemented testbed

The experimental testbench is shown in Fig. 4. A supercapacitor cell (from Maxwell Technologies®) with rated voltage and capacitance of 2.7V and 350F, respectively is used in the experiments. Detailed information about the parameters of the utilized supercapacitor cell is provided in the APPENDIX. In order to generate the desired current profiles and to emulate the real-life Electric Vehicle (EV) driving conditions, a closed-loop buck converter and a DC electronic load are implemented. The closed-loop buck converter controls the supercapacitor charge current. Likewise, the DC electronic load controls the discharge current of the supercapacitor. The DC electronic load is realized by closed-loop control of the gate-source voltage of a linear MOSFET (IXTK90N25L2), which is cascaded with a resistive load. The Digital Signal Processor (DSP) TMS320F28335 is used for closed-loop control of the converters. The PI controllers for current regulation and the algorithm of the proposed UKF-based approach for estimation of the supercapacitor SoH and SoE are realized in MATLAB/SIMULINK. The experiments are performed at room temperature ($T=25^\circ\text{C}$). The ACS712ELCTR-20A-T current sensor is used for measuring the supercapacitor charge/discharge current. In addition, the supercapacitor voltage is directly read by 12-bits ADC unit of the microprocessor. A sampling frequency of $f_s=1$ kHz is selected. A complete list of the experimental parameters is provided in Table I.

TABLE I
EXPERIMENTAL PARAMETERS OF THE TEST SYSTEM

Parameter	Value
Supercapacitor cell	Maxwell D-Cell®
Rated voltage of cell	2.7 V
Rated capacitance of cell	350 F
Current sensor	ACS712ELCTR-20A-T
Controller unit	TMS320F28335
Sampling frequency f_s	1 kHz
Operating temperature T	25 °C

B. Results and Discussions

In order to test the proposed UKF-based method, a number of scenarios are considered. Based on the charging/discharging current profiles that may occur in a real EV drive cycle, three scenarios are examined as follows:

Case A: In this case, the initial SoE of the supercapacitor is set to zero ($SoE_{initial} = 0$) and the supercapacitor gets charged

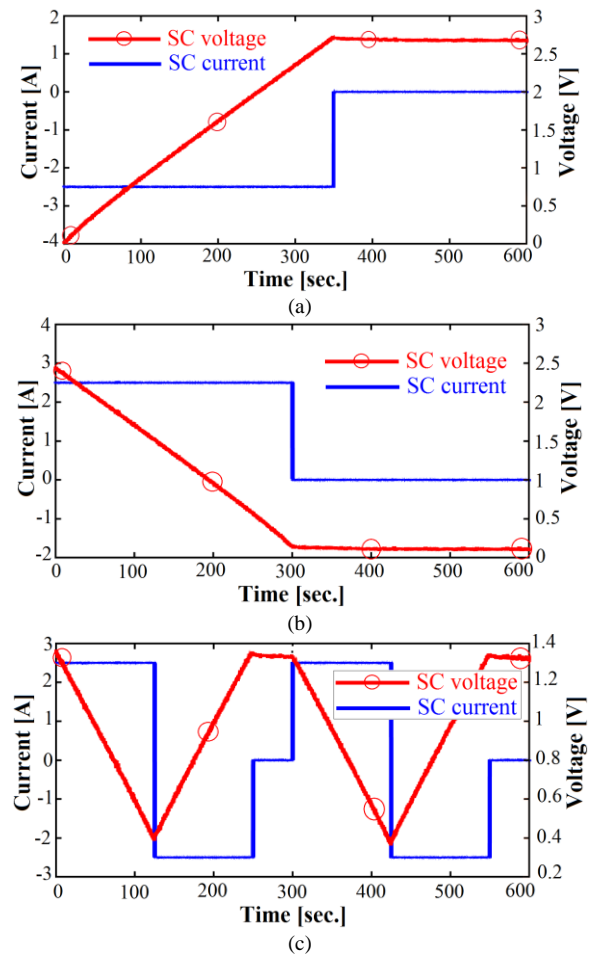


Fig. 5. Current and voltage profiles of the supercapacitor in scenarios A to C. (a) Scenario A. (b) Scenario B. (c) Scenario C

with constant current $i = -2.5\text{A}$. This case simulates the regenerative braking or EV coasting.

Case B: In this case, the initial SoE of the supercapacitor is set to 90% ($SoE_{initial} = 90\%$) and the supercapacitor gets discharged with constant current $i = +2.5\text{A}$. This case emulates the vehicle acceleration mode, in which the supercapacitor gets discharged to support the main energy storage unit.

Case C: In this case, the initial SoE is set to 50% ($SoE_{initial} = 50\%$). The supercapacitor is first discharged with $i = +2.5\text{A}$ and then, it is charged with $i = -2.5\text{A}$ followed by a rest condition for $\Delta t = 50$ seconds. The pattern is repeated twice during the experimentation time $\Delta t = 600$ seconds.

The charging/discharging current profiles in Cases A to C are depicted in Fig. 5. In Case A, the charging process is stopped when the cell is fully charged to 2.7V. Likewise, in Case B, the discharge current is set to zero (the load is disconnected) when the cell is fully discharged. To assess the robustness of the proposed approach against the measurement noises and errors, a fourth case (Case D) is also considered, which is similar to Case A except that band-limited white noise with a signal to noise ratio (SNR) of 30dB is added to the current and voltage measurements. In order to assess the accuracy of the proposed UKF-based estimator, the electrochemical impedance spectroscopy (EIS) method is used

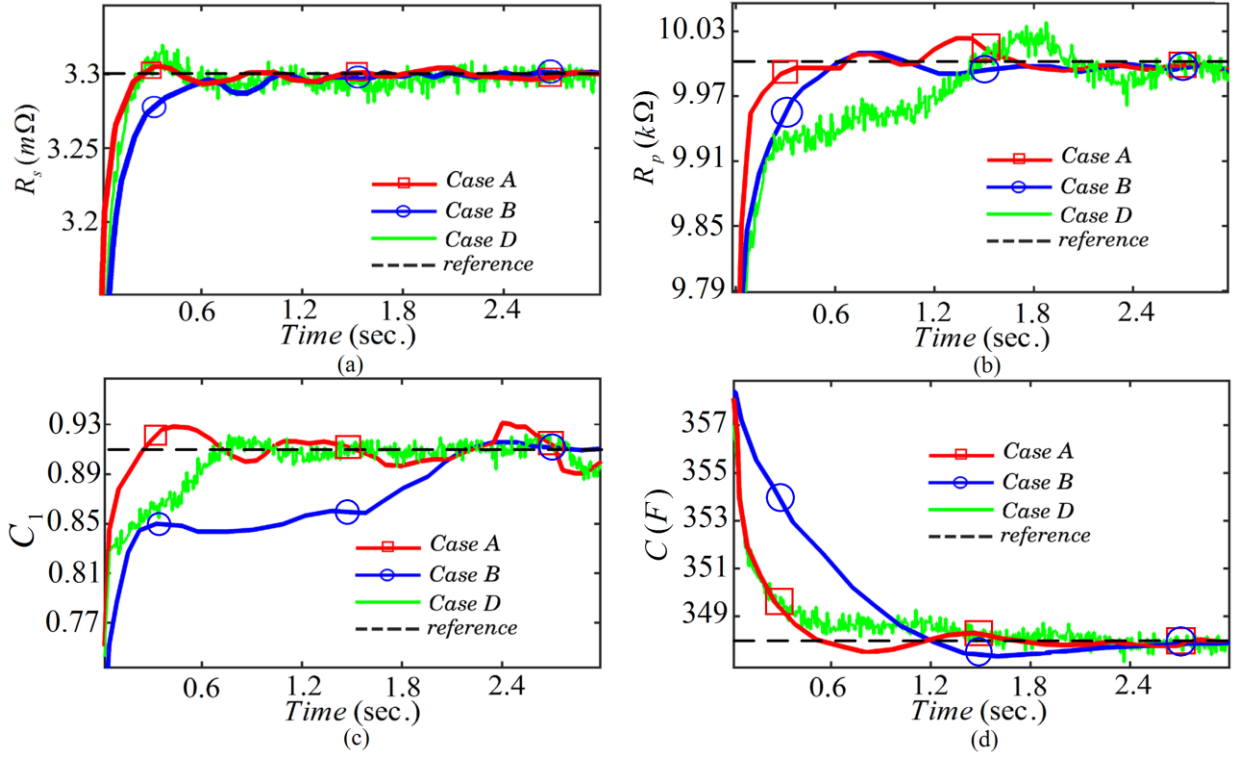


Fig. 6. State estimation results with the proposed UKF-based approach for cases A, B, and D. (a) Estimation results for R_s . (b) Estimation results for R_p . (c) Estimation results for C_1 . (d) Estimation results for C

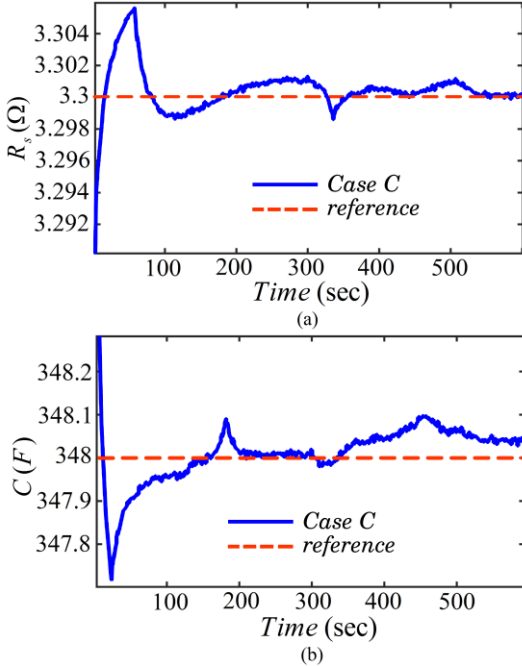


Fig. 7. Estimated SoH indicators with the proposed approach in Case C

as a benchmark. The obtained parameters of the supercapacitor model are as follows:

$$\begin{bmatrix} R_s & R_p & C_1 & C_0 \end{bmatrix}^T = \begin{bmatrix} 3.3m\Omega & 10k\Omega & 0.91 & 348F \end{bmatrix}^T$$

The supercapacitor states R_s and C reflect the SoH. The estimation accuracy of these parameters is assessed using the following formula:

$$SoH \text{ indicators errors } \% = \frac{x_{estimated} - x_{EIS}}{x_{EIS}} \times 100 \quad (26)$$

where x is either of the SoH indicators (R_s or C), $x_{estimated}$ is the estimated value of the state, and x_{EIS} is the real value of the system state obtained using the EIS. Furthermore, the estimation accuracy of SoE is calculated using the following formula:

$$SoE \text{ error } \% = \frac{SoE_{estimated} - SoE_{real}}{SoE_{real}} \times 100 = \frac{E_{estimated} - E_{real}}{E_{real}} \times 100 \quad (27)$$

where $SoE_{estimated}$ and $E_{estimated}$ are the estimated SoE and estimated supercapacitor remaining energy, respectively. In addition, SoE_{real} and E_{real} are the real SoE and remaining energy of the supercapacitor, respectively. E_{real} is obtained as follows:

$$E_{real} = E_0 + \underbrace{\int (i \times U_c) dt}_{\text{input energy}} - \underbrace{\left(\int R_s i^2 dt + \int \frac{v_c^2}{R_p} dt \right)}_{\text{energy loss}} \quad (28)$$

where E_0 is the initial stored energy of the supercapacitor. The state estimation results for Cases A, B, and D are shown in Fig. 6. Due to the space limit, only the results related to x_3 - x_6 are given. As seen, under no circumstance, the maximum convergence time of the proposed UKF-based estimator exceeds 1.5 seconds. In addition, the average error (calculated using (26) over a time period of 5 seconds after the convergence of the filter) for estimating the SoH indicators R_s and C , are $\approx 0.52\%$ and $\approx 0.32\%$, respectively. It can be seen that even when the measurements are contaminated with random noise with SNR of up to 30dB, the SoH indicators are accurately estimated. The faster convergence time in Case A is obtained

TABLE II

STATE ESTIMATION ERRORS OF SoE FOR DIFFERENT SCENARIOS

Scenario	Case A	Case B	Case C	Case D
SoE error %	0.473 %	0.512%	0.621%	0.813%

since the selected initial SoE in Case A is closer to the real initial state vector in the UKF algorithm. The estimated SoH indicators in Case C are also shown in Fig. 7. It can be deduced that the proposed estimator effectively estimates the supercapacitor parameters in different charging/discharging modes.

In Fig. 8, the results of the SoE estimation in Cases A, B, and C are depicted. It can be observed that in all Cases the SoE is accurately estimated. At the beginning stages of Cases B and C, relatively large differences between the estimated and real SoE are observable, which is due to the fact that the initial SoE of the supercapacitor in Cases B and C is set to 90% and 50%, respectively, which is different from the considered initial SoE of 0% in the UKF algorithm. However, it is seen that the SoE successfully converges to its reference value in a very short duration. The results also reveal that during the rest periods when the supercapacitor charging/discharging is terminated, the SoE gradually decreases due to the self-discharge effect caused by the parallel resistance in the supercapacitor model. The state estimation errors of the supercapacitor SoE in Cases A-D are also calculated using (27)-(28) and are summarized in Table II, which reports the mean error values over the simulation time. The results show that the error of the SoE estimation does not exceed 1% in the worst case when the measurement data are contaminated with random noise with SNR of up to 30dB.

IV. REAL-TIME FEASIBILITY DEMONSTRATION WITH HARDWARE-IN-THE-LOOP EXPERIMENTS

In order to demonstrate the real-time feasibility of the proposed UKF-based approach, a series of HIL experiments are conducted. The photo of the HL test is shown in Fig. 9. The proposed UKF-based method is completely implemented in MATLAB/SIMULINK environment. Therefore, the C code of the algorithm is first generated with MATLAB CODER option. The generated C code of the UKF algorithm is then downloaded to the 150 MHz DSP TMS320F28335 from Texas Instruments using Code Composer Studio 6.2.0 software. A pre-recorded dataset which includes the supercapacitor voltage and current signals is imported to MATLAB in a host computer. The current and voltage waveforms are contaminated with random Gaussian White noise with SNR of 30dB to effectively mimic the real-life conditions. The obtained voltage and current data are then sent from the host computer to the DSP in an online manner using the PCI-1712 data-acquisition card. In the meanwhile, analog low pass antialiasing filters of order two with a cut-off frequency of 2kHz are used. Upon receiving each data sample by DSP, the supercapacitor SoH and SoE are estimated with the proposed algorithm. The results are finally sent back to the host computer for monitoring and controlling purposes (to synchronize the whole HIL process). The required memory for the proposed UKF-based estimator is about 27kbytes, which is far lower than the memory of TMS320F28335 (256K×16 flash memory). Furthermore, the maximum run-time of the algorithm for the estimation is about 0.091 milliseconds. A sampling frequency of 1kHz is selected

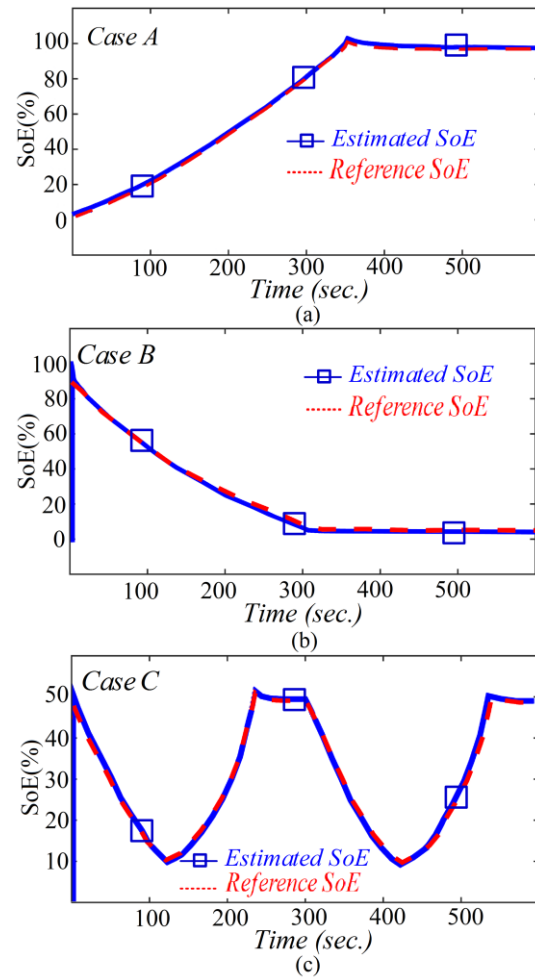


Fig. 8. Estimated SoE with the proposed UKF-based approach (a) Case A (b) Case B (c) Case C

for the algorithm (which is sufficiently good for state estimation in vehicular applications) and thus, each iteration must be accomplished within 1 millisecond. Therefore, only 9.1% of the processor resources will be used by the proposed algorithm and there will be no bottleneck for real-time implementation of the algorithm.

V. COMPARISON WITH SIMILAR METHODS

In this Section, a comparison between the proposed method with other KF-based approaches in terms of accuracy and computational complexity is presented. The results are summarized in Table III. The comparison reveals that the proposed UKF-based approach provides better accuracy for supercapacitor SoH and SoE estimation in comparison with KF-based and EKF-based methods. In addition, the computational burden of the proposed approach is lower than

TABLE III

COMPARISON BETWEEN THE PROPOSED METHOD AND KF-BASED ALGORITHMS

Method	SoH Accuracy	SoE Accuracy	CPU usage
KF-based [16]	≈98%	≈99%	5.2%
EKF-based [17]	≈95%	×	13.5%
UKF-based (proposed)	≈99.58%	≈99.4%	9.1%

× denotes that the estimation is not considered. All algorithms are tested using TMS320F28335 with sampling frequency of 1kHz

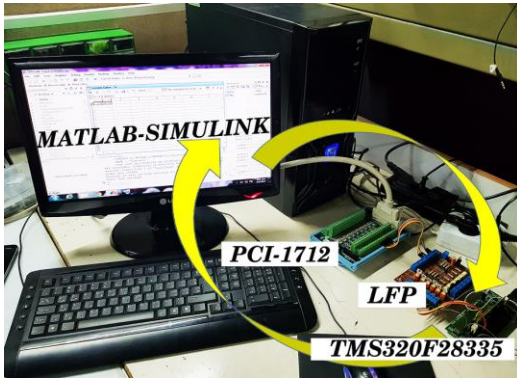


Fig. 9. Photo of the testbench for HIL tests

TABLE A
RATED VALUES OF THE UNDER-STUDY SUPERCAPACITOR CELL

Parameter	Value
Rated capacitance	350 F
Rated voltage	2.7 V
Absolute maximum voltage	2.85 V
Equivalent series resistance	3.2 mΩ
Leakage current (at $T=25^{\circ}\text{C}$)	0.3 mA
Specific energy	5.9 Wh/kg
Maximum continuous current	21 A

the EKF method, though the KF-based method still has the lowest computational complexity.

VI. CONCLUSION

A state estimation approach based on the UKF algorithm for joint estimation of the supercapacitor SoH and SoE is proposed in this paper. A first-order equivalent circuit model which takes into account the self-discharge and capacitance variation effects is developed. The supercapacitor model parameters and its internal voltage are augmented in one state-space model for concurrent estimation of SoH and SoE using the UKF algorithm. Unlike the KF and EKF algorithms which involve using a linearized supercapacitor model, the proposed UKF-based method achieves higher accuracy due to the use of nonlinear supercapacitor dynamics. Moreover, it effectively deals with the issues relevant to the measurement errors and modeling uncertainties with the involvement of covariance matrices of the measurement and process noise. While the proposed approach achieves higher accuracy than the state of art, its computational burden is remarkably low, which makes it a good candidate for real-time vehicular applications.

APPENDIX

The supercapacitor cell used for study is a Maxwell 350F radial D-Cell[®]. The rated values of the cell are provided in Table A.

ACKNOWLEDGMENT

This work has been supported by the French ministry of foreign affairs and the ministry of research and higher education of France, and the Iranian ministry of science research and technology, Center for International Scientific Studies and Cooperation (CISSC), within the frame of Gundishapur program.

REFERENCES

- [1] F. Naseri, E. Farjah, and T. Ghanbari, "An efficient regenerative braking system based on battery/supercapacitor for electric, hybrid, and plug-in hybrid electric vehicles with BLDC motor," *IEEE Transactions on Vehicular Technology*, vol. 66, no. 5, pp. 3724-3738, 2017.
- [2] A. Alessandrini, R. Barbieri, L. Berzi, F. Cignini, A. Genovese, E. Locorotondo, F. Ortenzi, M. Pierini, and L. Pugi, "Design of a Hybrid Storage for Road Public Transportation Systems," *International Conference of IFTO MM ITALY*, pp. 149-157, 2018.
- [3] J. Cao, and A. Emadi, "A new battery/ultracapacitor hybrid energy storage system for electric, hybrid, and plug-in hybrid electric vehicles," *IEEE Transactions on Power Electronics*, vol. 27, no. 1, pp. 122-132, 2012.
- [4] S. M. Lukic, J. Cao, R. C. Bansal, F. Rodriguez, and A. Emadi, "Energy storage systems for automotive applications," *IEEE Transactions on Industrial Electronics*, vol. 55, no. 6, pp. 2258-2267, 2008.
- [5] R. Köt, P. W. Ruch, and D. Cericola, "Aging and failure mode of electrochemical double layer capacitors during accelerated constant load tests," *Journal of power sources*, vol. 195, no. 3, pp. 923-928, 2010.
- [6] S. Buller, E. Karden, D. Kok, and R. W. De Doncker, "Modeling the dynamic behavior of supercapacitors using impedance spectroscopy," *IEEE Industry Applications Conference*, vol. 4, pp. 2500-2504, 2001.
- [7] P. Kreczanik, P. Venet, A. Hijazi, and G. Clerc, "Study of supercapacitor aging and lifetime estimation according to voltage, temperature, and RMS current," *IEEE Transactions on Industrial Electronics*, vol. 61, no. 9, pp. 4895-4902, 2014.
- [8] A. Soualhi, A. Sari, H. Razik, P. Venet, G. Clerc, R. German, O. Briat, and J. M. Vinassa, "Supercapacitors ageing prediction by neural networks," *IEEE Industrial Electronics Society Conference*, pp. 6812-6818, 2013.
- [9] A. Oukaour, M. Pouliquen, B. Tala-Ighil, H. Gualous, E. Pigeon, O. Gehan, and B. Boudart, "Supercapacitors aging diagnosis using least square algorithm," *Microelectronics Reliability*, vol. 53, no. 9, pp. 1638-1642, 2013.
- [10] N. Reichbach, and A. Kuperman, "Recursive-least-squares-based real-time estimation of supercapacitor parameters," *IEEE Transactions on Energy Conversion*, vol. 31, no. 2, pp. 810-812, 2016.
- [11] N. Reichbach, S. Kolesnik, and A. Kuperman, "Real-time state-of-energy estimation of supercapacitor-based energy storage," *IEEE East-West Design & Test Symposium*, pp. 1-4, 2015.
- [12] A. Eddahech, M. Ayadi, O. Briat, and J. M. Vinassa, "Online parameter identification for real-time supercapacitor performance estimation in automotive applications," *International Journal of Electrical Power & Energy Systems*, vol. 51, pp. 162-167, 2013.
- [13] F. Naseri, E. Farjah, M. Allahbakhshi, and Z. Kazemi, "Online condition monitoring and fault detection of large supercapacitor banks in electric vehicle applications," *IET Electrical Systems in Transportation*, vol. 7, no. 4, pp. 318-326, 2017.
- [14] M. Ceraolo, G. Lutzemberger, and D. Poli, "State-of-charge evaluation of supercapacitors," *Journal of Energy Storage*, vol. 11, pp. 211-218, 2017.
- [15] Y. Zhou, Z. Huang, H. Li, J. Peng, W. Liu, and H. Liao, "A Generalized Extended State Observer for Supercapacitor State of Energy Estimation with Online Identified Model," *IEEE Access*, 2018.
- [16] A. Nadeau, G. Sharma, and T. Soyata, "State-of-charge estimation for supercapacitors: A kalman filtering formulation," *IEEE International Conference on Acoustics, Speech and Signal Processing*, pp. 2194-2198, 2014.
- [17] A. El Mejdoubi, A. Oukaour, H. Chaoui, Y. Slamani, J. Sabor, and H. Gualous, "Online supercapacitor diagnosis for electric vehicle applications," *IEEE Transactions on Vehicular Technology*, vol. 65, no. 6, pp. 4241-4252, 2016.
- [18] A. Nadeau, M. Hassanaliagh, G. Sharma, T. Soyata, "Energy awareness for supercapacitors using Kalman filter state-of-charge tracking," *Journal of Power Sources*, vol. 296, pp. 383-391, 2015.
- [19] E. Locorotondo, L. Pugi, L. Berzi, M. Pierini, and A. Pretto, "Online State of Health Estimation of Lithium-Ion Batteries Based on Improved Ampere-Count Method," *IEEE International Conference on Environment and Electrical Engineering and 2018 IEEE Industrial and Commercial Power Systems Europe*, pp. 1-6, 2018.
- [20] E. Locorotondo, L. Pugi, L. Berzi, M. Pierini, and G. Lutzemberger, "Online Identification of Thevenin Equivalent Circuit Model Parameters and Estimation State of Charge of Lithium-Ion Batteries," *IEEE International Conference on Environment and Electrical*

Engineering and 2018 IEEE Industrial and Commercial Power Systems Europe, pp. 1-6, 2018.

- [21] W. Li, G. Joós, and J. Bélanger, "Real-time simulation of a wind turbine generator coupled with a battery supercapacitor energy storage system," *IEEE Transactions on Industrial Electronics*, vol. 57, no. 4, pp. 1137-1145, 2010.
- [22] N. Kularatna, J. Fernando, A. Pandey, and S. James, "Surge capability testing of supercapacitor families using a lightning surge simulator," *IEEE Transactions on Industrial Electronics*, vol. 58, no. 10, pp. 4942-4949, 2011.
- [23] Y. Y. Liu, J. J. Slotine, and A. L. Barabási, "Observability of complex systems," *Proceedings of the National Academy of Sciences*, vol. 110, no. 7, pp. 2460-2465, 2013.
- [24] F. Naseri, Z. Kazemi, M. M. Arefi, and E. Farjah, "Fast discrimination of transformer magnetizing current from internal faults: an extended Kalman filter-based approach," *IEEE Transactions on Power Delivery*, vol. 33, no. 1, pp. 110-118, 2018.
- [25] F. Naseri, Z. Kazemi, E. Farjah, and T. Ghanbari, "Fast Detection and Compensation of Current Transformer Saturation Using Extended Kalman Filter," *IEEE Transactions on Power Delivery*, 2019.
- [26] T. Ghanbari, E. Farjah, F. Naseri, N. Tashakor, H. Givi, and R. Khayam, "Solid-State Capacitor Switching Transient Limiter based on Kalman Filter algorithm for mitigation of capacitor bank switching transients," *Renewable and Sustainable Energy Reviews*, 2018.
- [27] D. Simon, "Optimal state estimation: Kalman, H infinity, and nonlinear approaches," John Wiley & Sons, 2006.



Farshid Naseri received the B.Sc. degree in electrical engineering from Shiraz University of Technology, Shiraz, Iran, in 2013, and the M.Sc. degree in electrical power engineering from Shiraz University, Shiraz, Iran, in 2015. He is now pursuing the Ph.D. degree in electrical power engineering in the Shiraz University. Currently, Farshid is a guest Ph.D. student at the Department of Energy Technology, Aalborg University, Aalborg, Denmark where he has joined the Electro-Mobility and Industrial Drives research program. His research interests include power electronics, electric vehicles, and state estimation.



Ebrahim Farjah received the B.Sc. degree in electrical and electronics engineering from Shiraz University, Iran, in 1987, the M.Sc. degree in electrical power engineering from Sharif University of Technology, Tehran, Iran, in 1989, and the Ph.D. degree in electrical engineering from Grenoble Institute of Technology, Grenoble, France. He is currently a Professor in the Department of Electrical and Computer Engineering of Shiraz University. His research interests include power electronics, renewable energy, micro-grids, and power quality.



Teymoor Ghanbari received the B.Sc. degree in Electrical Power Engineering from S.R. University, Tehran, Iran, the M.Sc. degree from Shahrood University of Technology, Shahrood, Iran, and the Ph.D. degree in the same field from Shiraz University, Shiraz, Iran. He is currently an Associate Professor in the School of Advanced Technologies of Shiraz University. His research interests include distributed generation, power electronics, and electrical machines.



Zahra Kazemi received the B.Sc. degree in electrical engineering from Shiraz University of Technology, Shiraz, Iran, in 2013, and the M.Sc. degree in control engineering from Shiraz University, Shiraz, Iran, in 2015. She is pursuing the Ph.D. degree in control engineering in the Shiraz University. Her research interests include system identification and modeling, industrial control and automation, machine learning, fault detection and fault diagnosis.



Erik Schaltz received the M.Sc. and Ph.D. degrees in electrical engineering from the Department of Energy Technology, Aalborg University, Aalborg, Denmark, in 2005 and 2010, respectively. From 2009 to 2012, he was working as an Assistant Professor with the Department of Energy Technology, Aalborg University, where he is currently working as an Associate Professor. At the department, he is the Programme Leader of the research programme in e-mobility and industrial drives and the Vice Programme Leader of battery storage systems. His research interests include analysis, modeling, design, and control of power electronics, electric machines, energy storage devices including batteries and ultracapacitors, fuel cells, hybrid electric vehicles, thermoelectric generators, reliability, and inductive power transfer systems.



Jean-Luc Schanen was born in 1968. He received the Diploma in electrical engineering and the Ph.D. degree from Grenoble Institute of Technology, Grenoble, France, in 1990 and 1994, respectively. He has been a Professor with the Grenoble Institute of Technology since 2003 and is leading the Power Electronics Research Group of the G2ELab. He is also the Deputy Director of the Engineering School of Energy, Water, and Environment. His research activities include the technological design of power electronics systems, including EMC aspects. His group develops models and tools for power converters optimization.